ACS OMEGA

http://pubs.acs.org/journal/acsodf

Article

Generating Bulk Nanobubbles in Alcohol Systems

Yuwen Ji, Zhen Guo, Tingyuan Tan, Yujiao Wang, Lijuan Zhang, Jun Hu, and Yi Zhang*

Cite This: *ACS Omega* 2021, 6, 2873−2881

Read Online

ACCESS | Metrics & More | Article Recommendations

ABSTRACT: Bulk nanobubbles (NBs) have attracted wide attention due to their peculiar physicochemical properties and great potential in applications in various fields. However, so far there are no reports on bulk NBs generated in pure organic systems, which we think is very important as NBs would largely improve the efficiency of gas−liquid mass transfer and facilitate chemical reactions to take place. In this paper, we verified that air and N_2 NBs could be generated in a series of alcohol solutions by using various methods including acoustical cavitation, pressurization−depressurization, and vibration. The experiments proved that NBs existed in alcohol solutions, with a highest density of 5.8×10^7 bubble/mL in propanol. Our results also indicated that bulk NBs could stably exist for at least hours in alcohol systems. The parameters in generating NBs in alcohols were optimized. Our findings open up an opportunity for improving gas−liquid mass transfer efficiency in the field of the chemical industry.

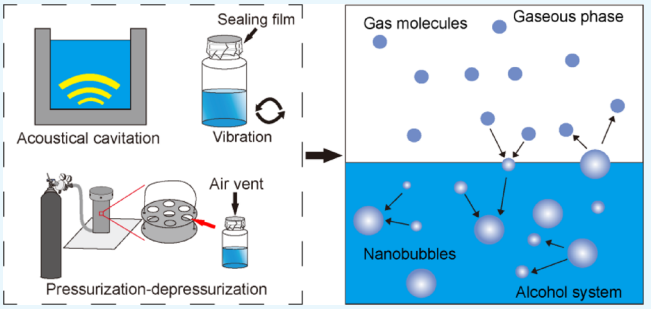

1. INTRODUCTION

Nanobubbles (NBs) are a new class of nanoscale systems that exist in solutions.[1−4] NBs have strong affinity for hydrophobic surfaces, extra-large wetting angle,[5,6] high water−gas interface area per unit of liquid volume, and long-term stability for several days even weeks.[7,8] Although many fundamental scientific questions in the NB field still remain unanswered, e.g., the amazing longevity of NBs in experimental observations in sharp contrast to ultrashort lifetimes predicted from the classical theories[9] and commented in recent publications.[10,11] NBs have shown great potential in applications for nanoscopic cleaning,[12] control of boundary slip in microfluidics,[13] wastewater treatment,[14] medical applications,[15] and so on.

Various methods for producing NBs have recently been developed, and evidences of the existence of NBs have been provided in a number of studies.[16−31,34−39] For instance, NBs were generated via chemical reactions[19] and by ultrasonic irradiation.[22] It was found that NBs could be produced through alcohol−water exchange, which was well characterized by the nanoparticle tracking analysis (NTA), Fourier transform infrared spectroscopy (FTIR), gas chromatography−mass spectrometry (GC−MS), and inductively coupled plasma-mass spectrometry (ICP-MS).[27] It was also reported that a procedure containing pressurization−depressurization steps would controllably generate NBs in different solutions, which was confirmed by the X-ray fluorescence intensity of the element of the gas in solutions and by NTA.[30] Although these independent studies provide strong evidence for the existence of NBs, they focus on aqueous solutions as liquid carriers. There is still debate on the existence of bulk NBs in a mixture of an organic solvent and water.[32,33] A few papers reported the formation of NBs in mixed systems.[34−37]

Due to the increasing contact surface area and long residence time of small-sized bubbles dispersed in liquid mediums, it is recognized that NBs would largely improve the efficiency of gas−liquid mass transfer.[40−42] If we could generate NBs in an organic liquid, the reaction between the gas and the organic liquid is expected to be largely promoted. Therefore, it is of great value to develop NBs in organic systems. At present, there are only few reports on whether NBs can be generated in pure organic systems. In 2004, Simonsen et al. observed surface NBs at the interface of pure alcohol and a hydrophobic silicon surface modified by polystyrene film but it was hard to reproduce.[43] Nirmalkar prepared NBs in different water−organic solvent systems by an acoustical cavitation method and suggested that hydroxide ions on the surface of aqueous solvents stabilized the NBs,[29] which was called the electrostatic repulsion model.[44] They pointed out that there were no ions on the surface of organic molecules, and NBs could not be formed in such a pure organic system.[30] Recent studies carried out by Barigou et al. also indicated that NBs were formed during water−organic solvent mixing, but no NBs were detected in pure organic systems.[27] However, it

Received: October 26, 2020
Accepted: December 1, 2020
Published: January 15, 2021

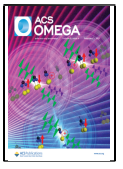

https://dx.doi.org/10.1021/acsomega.0c05222
ACS Omega 2021, 6, 2873−2881

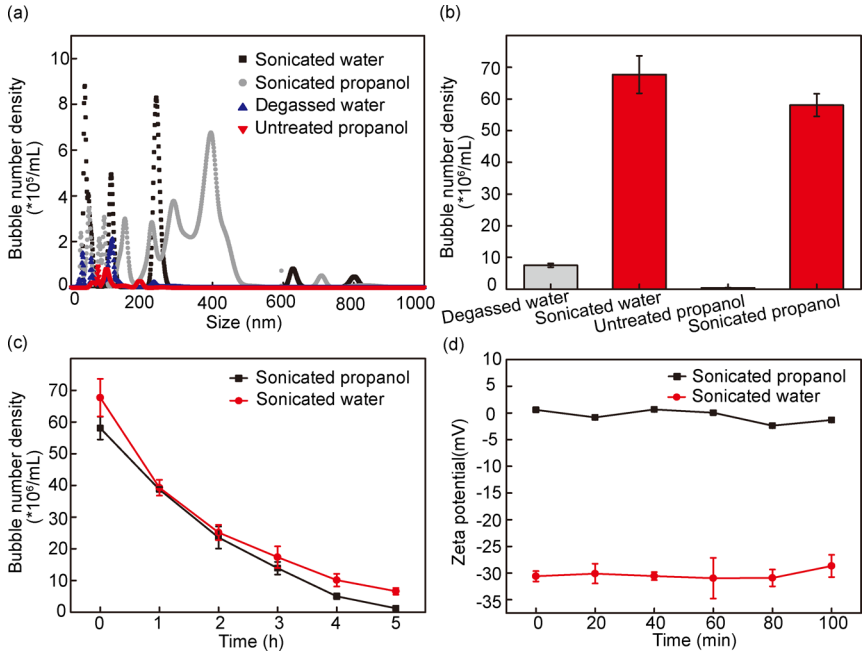

Figure 1. Characterization of bulk air NBs in propanol. (a) Size distributions of the ultrasonic cavitation-generated NBs in water and propanol; (b) histogram indicating the number density of NBs; (c) evolution of the number density of the ultrasonic cavitation-generated NBs in propanol and water during resting; (d) the change of zeta potential of the cavitation-generated air NBs in propanol and water over time.

seems that the electrostatic repulsion model does not work for bulk NBs in pure water (without surfactant) as the calculation showed that the repulsive pressure associated with electrostatic force caused by surface charge was one order of magnitude smaller than the Laplace pressure inside the bubble; thus, the electrostatic repulsive pressure could not balance with the Laplace pressure at all.[45,46] In 2015, Craig et al. observed the formation of surface NBs on highly oriented pyrolitic graphite (HOPG) covered by some pure organic solvents and believed the existence of a three-dimensional hydrogen bond network that promoted the formation of the surface NBs.[39] However, so far bulk NBs have not been produced in pure organic liquids.

Complicated interactions between the molecules of the gas phase and the organic solvent may be involved in a NB, especially at the gas−liquid interface. Therefore, properly selecting a suitable organic carrier for NB generation is very important for forming and stabilizing a NB in an organic solvent. Even though some scientists have explored the generation of NBs in organic solvent−water mixing systems, the types of organic solvents they studied and the methods they employed were very limited. In this paper, we systematically explored the possibility of generating bulk NBs in alcohol systems and demonstrated that either air or N_2 NBs could be indeed generated in these organic solvents via different preparation methods. Results indicated that air NBs in propanol could reach a number density of 5.8×10^7 bubble/mL, which is the largest one among the alcohol systems that we studied. Our results also indicated that bulk NBs could stably exist for at least hours in alcohol systems.

2. RESULTS AND DISCUSSION

2.1. Bulk Air NBs Prepared in Propanol by Acoustical Cavitation. Acoustical cavitation has been employed to prepare NBs in aqueous solutions.[16−18,31] Under ultrasonic irradiation, the generation and reduction of NBs in liquids occurred simultaneously, and the bubble core grows into cavitation bubbles through the expansion and compression of NBs. Cavitation bubbles break into tiny bubbles of various sizes, such as bubble nuclei and NBs.[22] In order to verify whether NBs can be generated in the alcohol systems, propanol solution and ultrapure water were sonicated and their results were compared. Ultrapure water was frozen at −20 °C for 8 h, whereafter it was degassed with melting at 0.1 atm and room temperature for 12 h, followed by cycling three times to obtain degassed water. Degassed water and untreated propanol were taken as controls. Figure 1a shows typical size distributions of air NBs in different samples. The peaks in the distribution curves represent respectively the highest populations of specific-sized individual bubbles and clusters of smaller bubbles,[47,48] which may change slowly over time, a phenomenon that is consistent with that reported in recent studies.[48,49] It was clear that there were very little NBs in degassed water (8×10^6 bubble/mL), while air NBs were almost undetectable in an untreated propanol solution (Figure 1b). After sonication treatment, the number density of NBs in propanol reached a value of $\sim 5.8 \times 10^7$ bubble/mL (Figure 1b). For comparison, the number density of air NBs in water treated with the same procedures was $\sim 6.7 \times 10^7$ bubble/mL (Figure 1b). From Figure 1a, the size of air NBs in the sonicated propanol solution was mostly in the range of 200−400 nm, while that in sonicated water was in 0−250 nm, indicating the size of NBs formed in propanol was generally larger than that in the aqueous system.

Bulk NBs in aqueous solutions have been reported to be stable for days or even weeks.[50−52] Here, we studied the long-term stability of air NBs generated by the acoustical cavitation method in propanol by monitoring the evolution of the bubble number density over time. The prepared NB suspension was sealed in a 20 mL glass vial and was extracted for analysis at different time intervals under room temperature. As shown in Figure 1c, the NB density in propanol gradually decreased to

https://dx.doi.org/10.1021/acsomega.0c05222
ACS Omega 2021, 6, 2873−2881

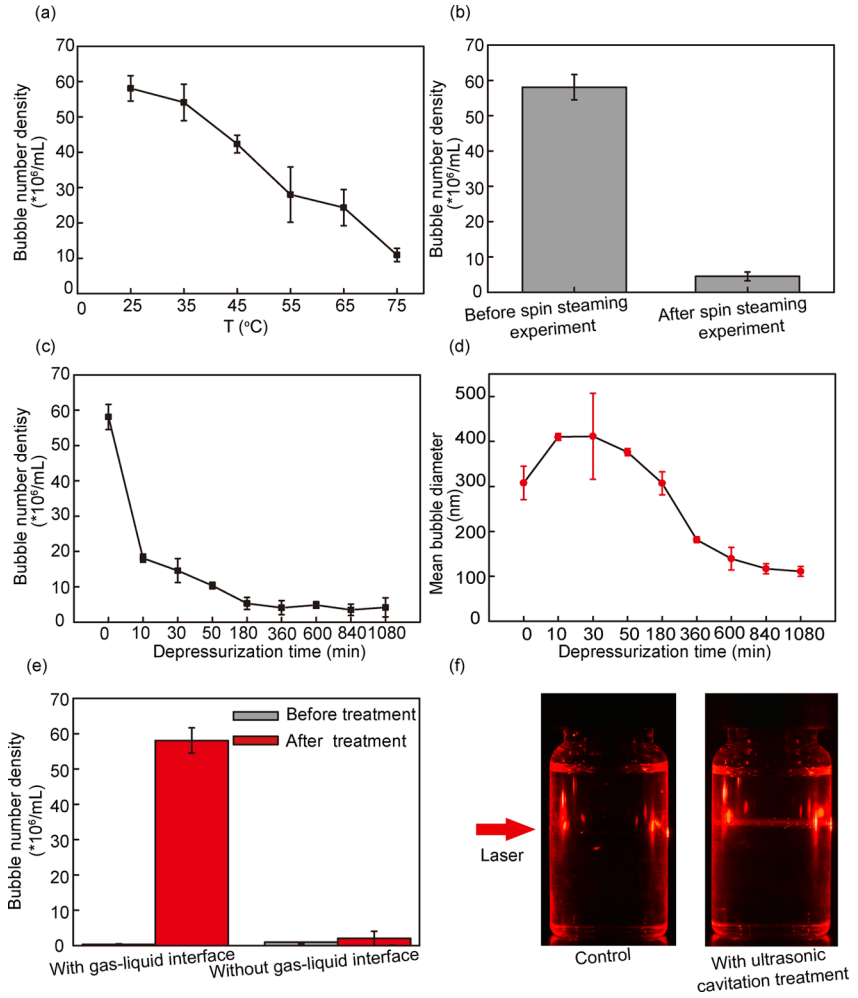

Figure 2. Verification of the NBs. (a) Number densities of ultrasonic cavitation-generated NBs operated at different temperatures; (b) the bubble and particle number densities before and after spin steaming experiment; (c) NB number density plotted against degassing time; (d) the change of mean NB diameter during degassing; (e) histogram indicating the number density of NBs plotted against the gas−liquid interface; (f) the scattering of a laser beam passing through the propanol solutions with and without ultrasonic cavitation treatment.

zero after 5 h, which indicated that the NBs have remarkable long-term stability in the alcohol system.

Zeta potential is a common method to measure surface charges of NB suspension in aqueous systems. Many scholars believe that negative charges on the NB's surface are one of the main factors stabilizing NBs by creating repulsive forces to prevent the coalescence of bubbles.[28,53,54] In order to explore the properties of the surface of the NBs formed in alcohol solutions, we measured the change of zeta potential in the air NB suspensions in propanol. As shown in Figure 1d, the zeta potential of NBs in propanol was stable around 0 mV over time in contrast to about −30 mV in water. Zero zeta potential on the air NBs in propanol may be due to that the propanol molecules are normally not ionized and cannot form negative charges on the surface of the NBs. Our results indicated that NBs could also be generated in propanol, which was hard to be ionized. Here, the zeta potential may refer to the potential at the interface of the gas phase and liquid propanol, in contrast to the potential at the electrical double-layer of the NBs in the water systems.[49]

The factors that stabilize the NBs in propanol still remain unclear. We think hydrogen bonds between the propanol molecules around the NBs may play a role. As propyl is hydrophobic and hydroxyl is hydrophilic, propanol molecules will be redistributed with propyl facing the gas phase and hydroxyl facing the liquid phase when the bulk NBs are formed.[55−57] In addition to weak C−H···O hydrogen bonds at the gas−liquid interface, the hydroxyl will form strong O−H···O hydrogen bonds with the adjacent propanol liquid.[58,59] Therefore, hydrogen bond strength in propanol containing bulk NBs will be higher than that in liquid propanol.

2.2. Verification of the Air NBs Generated in Propanol. *2.2.1. Heating.* Here, we indirectly verified that the nanoparticles detected by the NTA were NBs but not other nanoimpurities by means of heating. According to Henry's law, when the temperature goes up, the solubility of gas goes down. On the other hand, since organic solution is partially volatilized during the heating process, assuming the presence of other nanoscale impurities, heating will increase the density of detected nanoparticles rather than decreasing. In our experiments, when propanol solutions were treated by ultrasound under varied temperatures, it was found that the generated particles became less at the elevated temperatures (Figure 2a). The result ruled out the possibility that the particles produced by the ultrasonic method were contaminations. Rather, the decreased particle number upon heating complied with the characteristics of NBs.

https://dx.doi.org/10.1021/acsomega.0c05222
ACS Omega 2021, 6, 2873−2881

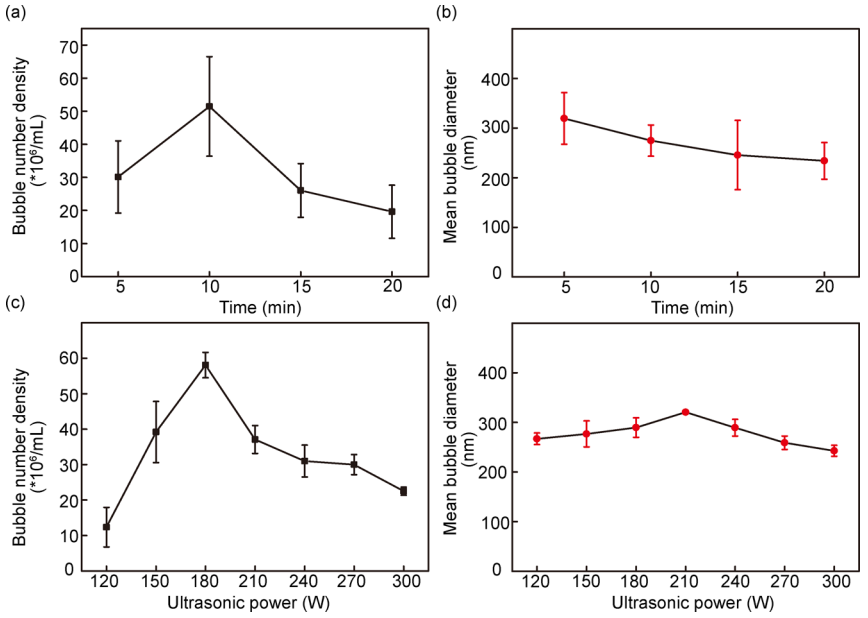

Figure 3. Optimization of conditions in an acoustical cavitation method. (a) Bubble number density plotted against the sonicating time; (b) mean diameter of the NBs plotted against the sonicating time; (c) bubble number density plotted against the sonicating power; (d) mean bubble diameter of the NBs plotted against the sonicating power.

2.2.2. Spin Steaming. The spin steaming experiment was to test what would happen when propanol solution was separated from NB suspensions. After NBs were generated, a flask that contained the NB suspension in propanol was placed in a rotary vacuum evaporator. The separation took place at 85 °C at vacuum (boiling) pressure. After evaporation of all propanol, analytical grade (99.9%) propanol was used to refill the flask trying to redissolve possible contaminations. As shown in Figure 2b, nearly no nanoscale impurities could be detected. This result further ruled out the possibility that the particles produced by the ultrasonic method were contaminations.

2.2.3. Degassing. A degassing process has been widely used as a simple way to verify the formation of NBs in solutions.[19,26,31] Since propanol can partly evaporate when exposed to low pressure for a long time, the concentration of nanoparticles detected by the NTA should increase if there are nano-impurities in the solution. In this experiment, we also conducted degassing experiments to figure out whether the nanoparticles detected by the NTA were indeed NBs. After degassing for 10 min under 0.1 atm, the number of sonication-generated air NBs in propanol dropped sharply (Figure 2c), a solid proof that the nanoparticles detected by the NTA were indeed NBs. The NB density was close to zero after further decompression for 18 h (Figure 2c). Interestingly, the mean diameter of the NBs changed during degassing (Figure 2d). The mean diameter of the NBs raised to its maximum (~400 nm) at 30 min and then gradually decreased to about 100 nm. The increase of the mean bubble diameter at the initial decompression stage may be a result of fusion of NBs in the propanol.

2.2.4. Ultrasonic Treatment without an Air/Liquid Interface. In the ultrasonic cavitation, air enters into the propanol from the gas/liquid interface. Therefore, there would be no air NBs formed during ultrasonic treatment without a gas−liquid interface.[31,60] In our experiment, 20 mL glass bottles were fully filled with propanol solution, therewith sealed with a lid to exclude the existence of a gas−liquid interface. As shown in Figure 2e, the bubble number density remained basically unchanged in such a case. It seems that, although propanol solution without a gas−liquid interface may be acoustically cavitated, no stabilized NBs were generated.

2.2.5. Tyndall Effect. The Tyndall effect is a direct way to distinguish colloids from solutions.[18,61,62] Ultrasonic cavitation-treated propanol was observed with the illumination of a red laser in a dark room. As shown in Figure 2f, a bright light revealing the scattering of the laser in the treated propanol was observed, a strong Tyndall effect that was not found in the untreated propanol solution. According the abovementioned verification experiments, the colloid particles that scattered the light were most likely NBs.

2.3. Optimization of Acoustical Ultrasonic Conditions. We think that the increase of the ultrasonic intensity and sonicating time would benefit the formation of NBs. However, an ultrasonic treatment with very high intensity and long treating time would led to fusion of small NBs into larger bubbles, resulting in the escape of gas from the solution. Next, optimal conditions including sonication time and ultrasonic power for generating air NBs in propanol with the acoustical cavitation method were explored. The results showed that a treatment time of 10 min would generate the highest NB density in propanol (Figure 3a) in the time range (5−20 min) that we studied. The mean diameter of the generated NBs fluctuated in the range of 230−320 nm and gradually decreased with the increase of sonicating time (Figure 3b). When the output power of the ultrasonic unit was set to 60% of its rated power (300 W), the density of the bubble number reached to a maximum value of ~5.8×10^7 bubble/mL (Figure 3c). The bubble diameter did not fluctuate significantly along with the change of the output power and reached its maximum at an output power of 70% rated power (Figure 3d).

2.4. Generating NBs in Propanol by Different Preparation Methods.[30,63] NBs in propanol were also generated by using the pressurization−depressurization method and vibration method. During the pressurization−

https://dx.doi.org/10.1021/acsomega.0c05222
ACS Omega 2021, 6, 2873−2881

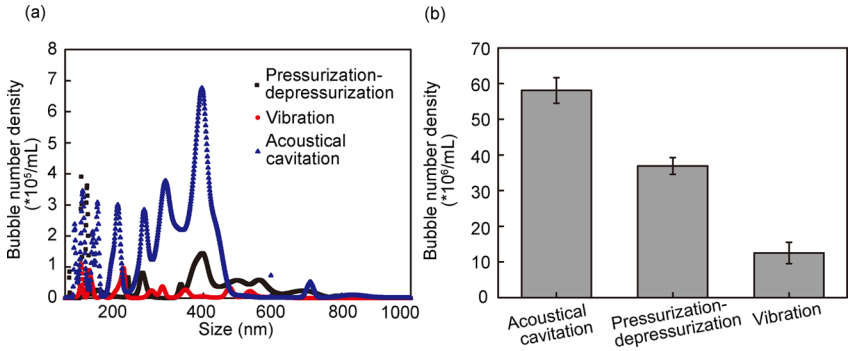

Figure 4. Generating NBs in propanol by different preparation methods (acoustical cavitation method: 10 min at 40 kHz output power of 180 W; pressurization−depressurization method: treated at a pressure of 2 MPa for 30 min and release of pressure at a rate of 0.33 MPa/h; vibration method: 3 min, 1800 r/min). (a) Distribution of bubble size; (b) bubble number density.

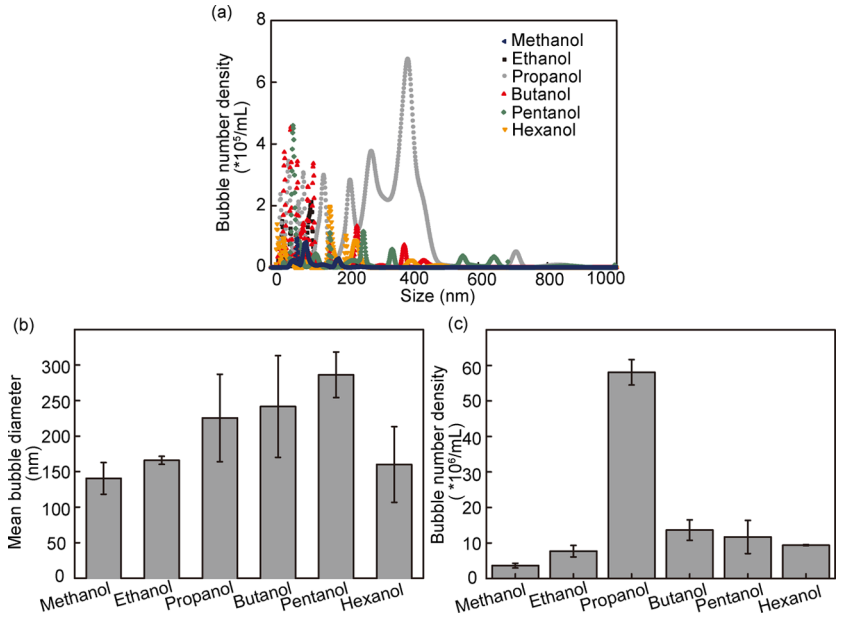

Figure 5. Air NBs generated in alcohols with different chain lengths by the acoustical cavitation method. (a) Distributions of bubble size; (b) mean bubble diameters; (c) bubble number densities.

depressurization process, the pressurization of the solvent increases the concentration of the dissolved gas, providing additional centers for gas nucleation, and the subsequent depressurization promotes uniform bubble nucleation. Meanwhile, in the vibration method, it mainly introduces more gases into organic solvents by speeding up the gas exchange at the gas−liquid interface. In this process, the formation of NBs has a complex relationship with the vibration time and frequency.

Figure 4 showed typical differences in bubble size distribution and bubble number density between NBs produced with different methods. The bubble number density in the pressurization−depressurization method reached a value of ∼3.7 × 10^7 bubble/mL, in contrast to ∼5.8 × 10^7 bubble/mL in the acoustical cavitation method and ∼1 × 10^7 bubble/mL in the vibration method. The experimental results indicated that the generation of NBs in propanol could be routinely achieved with various methods.

2.5. Bulk Air NBs Produced in Alcohols with Different Carbon Chain Lengths. Bulk air NBs were generated in alcohols with different carbon chain lengths by the acoustical cavitation method. Figure 5a showed typical NB size distributions varied with the length of the alcohol carbon chains. The result indicated that NBs in pentanol were the largest in size (Figure 5b), while the NBs in propanol had the largest bubble number density.

The trends in mean bubble diameter and bubble number density of the NBs in alcohols with different carbon chain lengths obtained by pressurization−depressurization (∼3.7 × 10^7 bubble/mL) and vibration methods (∼1 × 10^7 bubble/mL) were similar to those obtained by the acoustical cavitation method, as shown in Figure 6.

3. CONCLUSIONS

In summary, bulk NBs in alcohol systems have been successfully generated by using various methods. Our results indicated that bulk NBs could stably exist for at least hours in alcohol systems. Although trace impurities presented in alcohols might affect the light scattering measurements, our control experiments suggested that the colloidal particles that scattered the light were most likely bulk NBs. The highest number density of NBs varied in different alcohols that we studied, with a maximum value for the Propanol. The factors that stabilize the NBs in propanol still remain unclear. We think that hydrogen bonds between the propanol molecules

https://dx.doi.org/10.1021/acsomega.0c05222
ACS Omega 2021, 6, 2873−2881

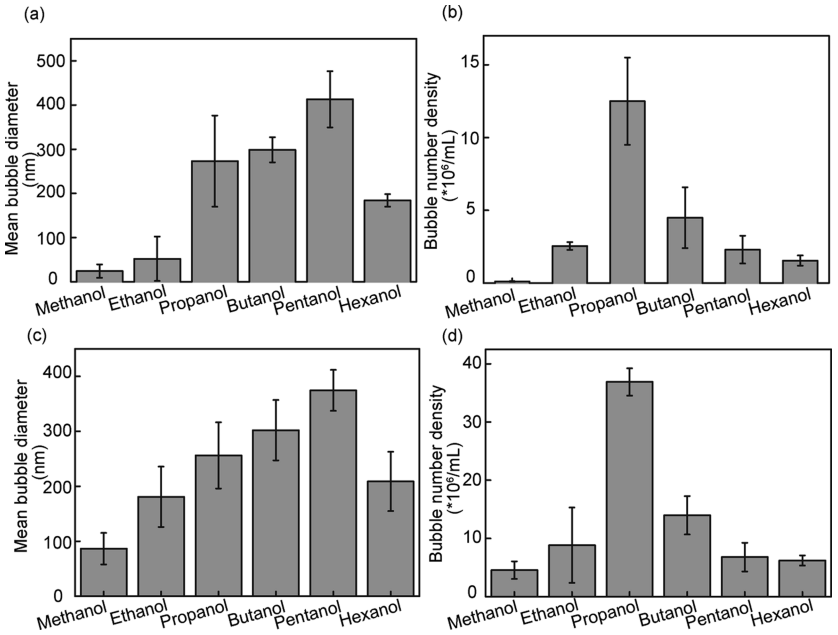

Figure 6. NBs produced in alcohols with different carbon chain lengths by different methods (pressurization−depressurization method: treated at a pressure of 2 MPa for 30 min and release of pressure at a rate of 0.33 MPa/h; vibration method: 3 min, 1800 r/min). (a) Mean bubble diameter of vibration-generated NBs. (b) Bubble number density of vibration-generated NBs; (c) mean bubble diameter of pressurization−depressurization-generated NBs; (d) bubble number density of pressurization−depressurization-generated NBs.

around the NBs may play a role. Our studies provided a possibility for increasing gas/liquid mass transfer efficiency through a NB formation route, which should have a great potential in increasing the reaction efficiency in a gas/liquid reaction.

4. MATERIALS AND METHODS

4.1. Materials. Alcohols including methanol, ethanol, propanol, butanol, pentanol, and hexanol (all in analytical grade, 99.9%) and sodium hydroxide (in analytical grade, ≥96.0%) were purchased from Sinopec Group Co., Ltd. Glassware was used in order to avoid contamination from plastic products. Ultrapure water from an ELGA LabWater (ELGA Classic-PURELAB) was used in all experiments. All solvents were examined by the NTA before use to insure that no nanoscale impurities within the measurable range of NTA could be detected.

4.2. Generating Air NBs in Alcohols by the Acoustical Cavitation Method.[20,22] The basic principle of NB generation is to create a local oversaturated state for gas and induce the nucleation of gas molecules. Here we used ultrasonic cavitation to nucleate air bubbles. When the ultrasonic intensity was higher than the "cavitation threshold", a small nucleus would be formed inside, and the dissolved gas was transferred to the small nucleus to form NBs. Briefly, a 20 mL glass bottle containing 5 mL alcohol solution was put in a water bath on a ultrasonic generator that was operated at a frequency of 40 kHz and 60% of its rated power (300 W). The temperature was set to 25 °C. In order to avoid contamination, the glass bottle was sealed by a piece of parafilm penetrated by a clean steel needle which bridged inner and outer sides of the bottle to allow air to circulate.

4.3. Generating N_2 NBs in Alcohols by the Pressurization−Depressurization Method.[30] The N_2 NBs were generated by precipitating out of the dissolved gas in the alcohol solutions. Experiments were performed under room temperature in a custom-made stainless chamber that controlled the pressure inside. First, a 20 mL glass bottle containing 5 mL of alcohol solution was placed in a pressurized chamber (2 MPa) for 30 min. Then, a depressurization process with a speed of 0.33 MPa/h was executed to decrease the pressure inside the chamber to the normal atmosphere (∼0.1 MPa). Detailed description of the experimental setup and procedures are available in a paper published previously.[30]

4.4. Generating Air NBs in Alcohols by the Vibration Method.[63] Alcohol solution (5 mL) in a 20 mL glass bottle was placed in a Talboys standard vortex mixer (Scientific Industries, Inc.), which was circularly oscillated at a range of 0−5400 rpm (r/min) for 3 min. In order to avoid contamination, the bottle was sealed with a parafilm. After the vibration, the NB suspension was left standing for 2 min so that larger bubbles visible to the naked eyes would burst and disappear.

4.5. NTA. The number density and size distribution of NBs were characterized by an NTA instrument (Nanosight, NS 300, Malvern), which is suitable for the real-time analysis of polydispersed particles ranging from 10 to 2000 nm in size and 10^6 to 10^9 particles/mL in number density. The NTA instrument was equipped with a 20-fold magnification microscope, a high-speed camera, and a 65 mW laser light source (405 nm). Each data was averaged from 10 individual measurements, and the film lasted 60 s, capturing at 25 frames/s. The camera level was usually set to 10, the threshold was set to 13, and the solution viscosity was 0.4−5 cP (mPa·s). During measurement, the optical field was fixed to about 80 μm, and the depth of the light beam was about 10 μm. The particle concentration could be obtained by dividing the volume of the field by the number of nanoparticles. The camera subsequently captured a video of the particles moving under Brownian motion within a field of view of approximately 100 μm × 80 μm × 10 μm. The size of nanoparticles was determined using the Stokes−Einstein equation:

https://dx.doi.org/10.1021/acsomega.0c05222
ACS Omega 2021, 6, 2873−2881

$$D_t = \frac{Tk_B}{3\pi\eta d}$$

where k_B, T, and η are the Boltzman constant, the temperature, and the liquid viscosity, respectively, and D_t is the diffusion coefficient, which is an experimentally measured value based on the Brownian motion of the particle.[62]

4.6. Zeta Potential. Zeta potential, also known as electric potential at the slip plane in the case of colloids, is an important indicator of the stability of colloidal dispersion systems. Zeta potential can be derived using a theoretical model and experimentally determined electrophoretic mobility of charged entities under an applied electric field. The electrophoretic mobility, μ_e, is defined as

$$\mu_e = \frac{u}{e}$$

where u is the drift velocity of the dispersed particle, and e is the strength of the applied electric field. Thus, the zeta potential, ζ, can be calculated from

$$\mu_e = \frac{2\varepsilon_r\varepsilon_0\zeta f(\kappa a)}{3\eta}$$

where ε_r, ε_0, η, and $f(\kappa a)$ are the relative permittivity or dielectric constant of the dispersion medium, the permittivity of vacuum, the dynamic viscosity of the dispersion medium at the experimental temperature, and Henry's function, respectively. Here, the zeta potential of the NB suspensions was measured by a Zetasizer Nano ZS 90 (Malvern Instruments, U.K.).[64,65]

AUTHOR INFORMATION

Corresponding Author

Yi Zhang − *Key Laboratory of Interfacial Physics and Technology, Shanghai Institute of Applied Physics, Chinese Academy of Sciences, Shanghai 201800, China; Zhangjiang Lab, Shanghai Advanced Research Institute, Chinese Academy of Sciences, Shanghai 201210, China;* orcid.org/0000-0003-2024-2624; Phone: +0086-21-39194607; Email: zhangyi@sinap.ac.cn; Fax: +0086-21-59552394

Authors

Yuwen Ji − *Key Laboratory of Interfacial Physics and Technology, Shanghai Institute of Applied Physics, Chinese Academy of Sciences, Shanghai 201800, China; University of Chinese Academy of Sciences, Beijing 100049, China*

Zhen Guo − *Key Laboratory of Interfacial Physics and Technology, Shanghai Institute of Applied Physics, Chinese Academy of Sciences, Shanghai 201800, China; University of Chinese Academy of Sciences, Beijing 100049, China*

Tingyuan Tan − *Key Laboratory of Interfacial Physics and Technology, Shanghai Institute of Applied Physics, Chinese Academy of Sciences, Shanghai 201800, China; University of Chinese Academy of Sciences, Beijing 100049, China*

Yujiao Wang − *Key Laboratory of Interfacial Physics and Technology, Shanghai Institute of Applied Physics, Chinese Academy of Sciences, Shanghai 201800, China; University of Chinese Academy of Sciences, Beijing 100049, China*

Lijuan Zhang − *Key Laboratory of Interfacial Physics and Technology, Shanghai Institute of Applied Physics, Chinese Academy of Sciences, Shanghai 201800, China; Zhangjiang Lab, Shanghai Advanced Research Institute, Chinese Academy of Sciences, Shanghai 201210, China*

Jun Hu − *Key Laboratory of Interfacial Physics and Technology, Shanghai Institute of Applied Physics, Chinese Academy of Sciences, Shanghai 201800, China; Zhangjiang Lab, Shanghai Advanced Research Institute, Chinese Academy of Sciences, Shanghai 201210, China;* orcid.org/0000-0002-7282-2316

Complete contact information is available at: https://pubs.acs.org/10.1021/acsomega.0c05222

Author Contributions

Y.J. contributed to the conceptualization, methodology, and investigation of the study and writing the original draft. Z.G. performed the formal analysis and investigation and contributed to reviewing & editing the paper. T.T. and Y.W. contributed to the methodology and investigation. L.Z. participated in the investigation and supervision and in reviewing & editing the paper. J.H. contributed to the conceptualization and in reviewing & editing the paper. Y.Z. contributed in reviewing & editing he paper and in conceptualization, methodology, supervision, and funding acquisition.

Notes

The authors declare no competing financial interest.

ACKNOWLEDGMENTS

This work was financially supported by the National Natural Science Foundation of China (nos. 11975297 and 11674344) and the Key Research Program of Frontier Sciences, CAS (grant no. QYZDJ-SSW-SLH019).

REFERENCES

(1) Parker, J. L.; Claesson, P. M.; Attard, P. Bubbles, Cavities, and the Long-Ranged Attraction between Hydrophobic Surfaces. *J. Phys. Chem.* **1994**, *98*, 8468−8480.

(2) Lou, S.-T.; Ouyang, Z.-Q.; Zhang, Y.; Li, X.-J.; Hu, J.; Li, M.-Q.; Yang, F.-J. Nanobubbles on Solid Surface Imaged by Atomic Force Microscopy. *J. Vac. Sci. Technol., B: Microelectron. Nanometer Struct.–Process., Meas., Phenom.* **2000**, *18*, 2573−2575.

(3) Ishida, N.; Inoue, T.; Miyahara, M.; Higashitani, K. Nano Bubbles on a Hydrophobic Surface in Water Observed by Tapping-Mode Atomic Force Microscopy. *Langmuir* **2000**, *16*, 6377−6380.

(4) Tyrrell, J. W. G.; Attard, P. Images of Nanobubbles on Hydrophobic Surfaces and Their Interactions. *Phys. Rev. Lett.* **2001**, *87*, 176104.

(5) Zhang, L.; Zhao, B.; Xue, L.; Guo, Z.; Dong, Y.; Fang, H.; Tai, R.; Hu, J. Imaging Interfacial Micro- and Nano-bubbles by Scanning Transmission Soft X-ray Microscopy. *J. Synchrotron. Rad.* **2013**, *20*, 413−418.

(6) Hu, J.; Xiao, X.-D.; Ogletree, D. F.; Salmeron, M. Imaging the Condensation and Evaporation of Molecularly Thin Films of Water with Nanometer Resolution. *Science* **1995**, *268*, 267−269.

(7) Azevedo, A.; Oliveira, H.; Rubio, J. Bulk Nanobubbles in the Mineral and Environmental Areas: Updating Research and Applications. *Adv. Colloid Interface Sci.* **2019**, *271*, 101992.

(8) Ball, P. How to Keep Dry in Water. *Nature* **2003**, *423*, 25−26.

(9) Epstein, P. S.; Plesset, M. S. On the Stability of Gas Bubbles in Liquid Gas Solutions. *J. Chem. Phys.* **1950**, *18*, 1505.

(10) Craig, V. S. J. Very Small Bubbles at Surfaces-the Nanobubble puzzle. *Soft Matter* **2011**, *7*, 40−48.

(11) Zhang, X.; Lohse, D. Perspectives on Surface Nanobubbles. *Biomicrofluidics* **2014**, *8*, No. 041301.

(12) Zhu, J.; An, H.; Alheshibri, M.; Liu, L.; Terpstra, P. M. J.; Liu, G.; Craig, V. S. J. Cleaning with Bulk Nanobubbles. *Langmuir* **2016**, *32*, 11203−11211.

(13) Wang, Y.; Bhushan, B. Boundary Slip and Nanobubble Study in Micro/Nanofluidics Using Atomic Force Microscopy. *Soft Matter* **2010**, *6*, 29−66.
(14) Agarwal, A.; Ng, W. J.; Liu, Y. Principle and Applications of Microbubble and Nanobubble Technology for Water Treatment. *Chemosphere* **2011**, *84*, 1175−1180.
(15) Modi, K. K.; Jana, A.; Ghosh, S.; Watson, R.; Pahan, K. A Physically-Modified Saline Suppresses Neuronal Apoptosis, Attenuates Tau Phosphorylation and Protects Memory in an Animal Model of Alzheimer's Disease. *PLoS One* **2014**, *9*, No. e103606.
(16) Nirmalkar, N.; Pacek, A. W.; Barigou, M. Interpreting the Interfacial and Colloidal Stability of Bulk Nanobubbles. *Soft Matter* **2018**, *14*, 9643−9656.
(17) Alheshibri, M.; Craig, V. S. J. Differentiating between Nanoparticles and Nanobubbles by Evaluation of the Compressibility and Density of Nanoparticles. *J. Phys. Chem. C* **2018**, *122*, 21998−22007.
(18) Michailidi, E. D.; Bomis, G.; Varoutoglou, A.; Kyzas, G. Z.; Mitrikas, G.; Mitropoulos, A. C.; Efthimiadou, E. K.; Favvas, E. P. Bulk Nanobubbles: Production and Investigation of Their Formation/Stability Mechanism. *J. Colloid Interface Sci.* **2020**, *564*, 371−380.
(19) Alheshibri, M.; Jehannin, M.; Coleman, V. A.; Craig, V. S. J. Does gas supersaturation by a chemical reaction produce bulk nanobubbles? *J. Colloid Interface Sci.* **2019**, *554*, 388−395.
(20) Mo, C. R.; Wang, J.; Fang, Z.; Zhou, L. M.; Zhang, L. J.; Hu, J. Formation and Stability of Ultrasonic Generated Bulk Nanobubbles. *Chin. Phys. B* **2018**, *27*, 118104.
(21) Nirmalkar, N.; Pacek, A. W.; Barigou, M. On the Existence and Stability of Bulk Nanobubbles. *Langmuir* **2018**, *34*, 10964−10973.
(22) Yasuda, K.; Matsushima, H.; Asakura, Y. Generation and Reduction of Bulk Nanobubbles by Ultrasonic Irradiation. *Chem. Eng. Sci.* **2019**, *195*, 455−461.
(23) Postnikov, A. V.; Uvarov, I. V.; Penkov, N. V.; Svetovoy, V. B. Collective Behavior of Bulk Nanobubbles Produced by Alternating Polarity Electrolysis. *Nanoscale* **2018**, *10*, 428−435.
(24) Qiu, J.; Zou, Z.; Wang, S.; Wang, X.; Wang, L.; Dong, Y.; Zhao, H.; Zhang, L.; Hu, J. Formation and Stability of Bulk Nanobubbles Generated by Ethanol-Water Exchange. *Chem. Phys. Chem.* **2017**, *18*, 1345−1350.
(25) Millare, J. C.; Basilia, B. A. Nanobubbles from Ethanol-Water Mixtures: Generation and Solute Effects via Solvent Replacement Method. *ChemistrySelect* **2018**, *3*, 9268−9275.
(26) Xiao, W.; Wang, X.; Zhou, L.; Zhou, W.; Wang, J.; Qin, W.; Qiu, G.; Hu, J.; Zhang, L. Influence of Mixing and Nanosolids on the Formation of Nanobubbles. *J. Phys. Chem. B.* **2018**, *123*, 317−323.
(27) Jadhav, A. J.; Barigou, M. Proving and Interpreting the Spontaneous Formation of Bulk Nanobubbles in Aqueous Organic Solvent Solutions: Effects of Solvent Type and Content. *Soft Matter* **2020**, *16*, 4502.
(28) Oh, S. H.; Kim, J. M. Generation and Stability of Bulk Nanobubbles. *Langmuir* **2017**, *33*, 3818−3823.
(29) Nirmalkar, N.; Pacek, A. W.; Barigou, M. Bulk Nanobubbles from Acoustically Cavitated Aqueous Organic Solvent Mixtures. *Langmuir* **2019**, *35*, 2188−2195.
(30) Ke, S.; Xiao, W.; Quan, N.; Dong, Y.; Zhang, L.; Hu, J. Formation and Stability of Bulk Nanobubbles in Different Solutions. *Langmuir* **2019**, *35*, 5250−5256.
(31) Fang, Z.; Wang, L.; Wang, X.; Zhou, L.; Wang, S.; Zou, Z.; Tai, R.; Zhang, L.; Hu, J. Formation and Stability of Surface/Bulk Nanobubbles Produced by Decompression at Lower Gas Concentration. *J. Phys. Chem. C* **2018**, *122*, 22418−22423.
(32) Sedlák, M.; Rak, D. Large-Scale Inhomogeneities in Solutions of Low Molar Mass Compounds and Mixtures of Liquids: Supramolecular Structures or Nanobubbles? *J. Phys. Chem. B.* **2013**, *117*, 2495−2504.
(33) Alheshibri, M.; Craig, V. S. J. Generation of nanoparticles upon mixing ethanol and water Nanobubbles or Not? *J. Colloid Interface Sci.* **2019**, *542*, 136−143.
(34) Jin, F.; Ye, J.; Hong, L.; Lam, H.; Wu, C. Slow Relaxation Mode in Mixtures of Water and Organic Molecules: Supramolecular Structures or Nanobubbles? *J. Phys. Chem. B.* **2007**, *111*, 2255−2261.
(35) Häbich, A.; Ducker, W.; Dunstan, D. E.; Zhang, X. Do Stable Nanobubbles Exist in Mixtures of Organic Solvents and Water? *J. Phys. Chem. B.* **2010**, *114*, 6962−6967.
(36) Jin, F.; Li, J.; Ye, X.; Wu, C. Effects of pH and Ionic Strength on the Stability of Nanobubbles in Aqueous Solutions of α-Cyclodextrin. *J. Phys. Chem. B.* **2007**, *111*, 11745−11749.
(37) Jin, F.; Ye, X.; Wu, C. Observation of Kinetic and Structural Scalings during Slow Coalescence of Nanobubbles in an Aqueous Solution. *J. Phys. Chem. B.* **2007**, *111*, 13143−13146.
(38) Ghaani, M. R.; Kusalik, P. G.; English, N. J. Massive Generation of Metastable Bulk Nanobubbles in Water by External Electric Fields. *Sci. Adv.* **2020**, *6*, eaaz0094.
(39) An, H.; Liu, G.; Atkin, R.; Craig, V. S. J. Surface Nanobubbles in Nonaqueous Media: Looking for Nanobubbles in DMSO, Formamide, Propylene Carbonate, Ethylammonium Nitrate, and Propylammonium Nitrate. *ACS Nano* **2015**, *9*, 7596−7607.
(40) Hu, B.; Nienow, A. W.; Stitt, E. H.; Pacek, A. W. Bubble Sizes in Agitated Solvent/Reactant Mixtures Used in Heterogeneous Catalytic Hydrogenation of 2-butyne-1,4-diol. *Chem. Eng. Sci.* **2006**, *61*, 6765−6774.
(41) Ye, Y.; Yu, S.; Hou, L.; Liu, B.; Xia, Q.; Liu, G.; Li, P. Microbubble Aeration Enhances Performance of Vacuum Membrane Distillation Desalination by Alleviating Membrane Scaling. *Water Res.* **2019**, *149*, 588−595.
(42) Liu, Y.; Yue, J.; Zhao, S.; Yao, C.; Chen, G. Bubble Splitting Under Gas-Liquid-Liquid Three-Phase Flow in a Double T-Junction Microchannel. *AIChE J.* **2018**, *64*, 376−388.
(43) Simonsen, A. C.; Hansen, P. L.; Klösgen, B. Nanobubbles Give Evidence of Incomplete Wetting at a Hydrophobic Interface. *J. Colloid. Interface Sci.* **2004**, *273*, 291−299.
(44) Bunkin, F. V. ON RADIATION IN ANISOTROPIC MEDIA. *Sov. Phys. JETP.* **1957**, *5*, 277−283.
(45) Kyuichi, Y. Mechanism for Stability of Ultrafine Bubbles. *Jpn. J. Multiphase Flow.* **2016**, *30*, 19−26.
(46) Yasui, K.; Tuziuti, T.; Kanematsu, W. Mysteries of Bulk Nanobubbles (Ultrafine bubbles); Stability and Radical Formation. *Ultrason. Sonochem.* **2018**, *48*, 259−266.
(47) Midtvedt, D.; Eklund, F.; Olsén, E.; Midtvedt, B.; Swenson, J.; Höök, F. Size and Refractive Index Determination of Subwavelength Particles and Air Bubbles by Holographic Nanoparticle Tracking Analysis. *Anal. Chem.* **2020**, *92*, 1908−1915.
(48) Ma, T.; Kimura, Y.; Yamamoto, H.; Feng, X.; Hirano-Iwata, A.; Niwano, M. Characterization of Bulk Nanobubbles Formed by Using a Porous Alumina Film with Ordered Nanopores. *J. Phys. Chem. B.* **2020**, *124*, 5067−5072.
(49) Ferraro, G.; Jadhav, A. J.; Barigou, M. A Henry's law method for generating bulk nanobubbles. *Nanoscale* **2020**, *12*, 15869.
(50) Weijs, J. H.; Seddon, J. R. T.; Lohse, D. Diffusive Shielding Stabilizes Bulk Nanobubble Clusters. *Chem. Phys. Chem.* **2012**, *13*, 2197−2204.
(51) Ohgaki, K.; Khanh, N. Q.; Joden, Y.; Tsuji, A.; Nakagawa, T. Physicochemical Approach to Nanobubble Solutions. *Chem. Eng. Sci.* **2010**, *65*, 1296−1300.
(52) Ebina, K.; Shi, K.; Hirao, M.; Hashimoto, J.; Kawato, Y.; Kaneshiro, S.; Morimoto, T.; Koizumi, K.; Yoshikawa, H. Oxygen and Air Nanobubble Water Solution Promote the Growth of Plants, Fishes, and Mice. *PLoS One* **2013**, *8*, No. e65339.
(53) Cho, S.-H.; Kim, J.-Y.; Chun, J.-H.; Kim, J.-D. Ultrasonic Formation of Nanobubbles and Their Zeta-potentials in Aqueous Electrolyte and Surfactant Solutions. *Colloids Surf., A* **2005**, *269*, 28−34.
(54) Tyrrell, J. W. G.; Attard, P. Atomic Force Microscope Images of Nanobubbles on a Hydrophobic Surface and Corresponding Force-Separation Data. *Langmuir* **2002**, *18*, 160−167.

https://dx.doi.org/10.1021/acsomega.0c05222
ACS Omega 2021, 6, 2873−2881

(55) Taylor, R. S.; Garrett, B. C. Accommodation of Alcohols by the Liquid/Vapor Interface of Water: Molecular Dynamics Study. *J. Phys. Chem. B.* **1999**, *103*, 844−851.
(56) Tarek, M.; Tobias, D. J.; Klein, M. L. Molecular dynamics investigation of an ethanol-water solution. *Phys. A* **1996**, *231*, 117−122.
(57) Stewart, E.; Shields, R. L.; Taylor, R. S. Molecular Dynamics Simulations of the Liquid/Vapor Interface of Aqueous Ethanol Solutions as a Function of Concentration. *J. Phys. Chem. B.* **2003**, *107*, 2333−2343.
(58) Tarek, M.; Tobias, D. J.; Klein, M. L. Molecular Dynamics Investigation of the Surface/Bulk Equilibrium in an Ethanol-Water Solution. *J. Chem. Soc., Faraday Trans.* **1996**, *92*, 559−563.
(59) Chen, B.; Siepmann, J. I.; Klein, M. L. Vapor-Liquid Interfacial Properties of Mutually Saturated Water/1-Butanol Solutions. *J. Am. Chem. Soc.* **2002**, *124*, 12232−12237.
(60) Filipe, V.; Hawe, A.; Jiskoot, W. Critical Evaluation of Nanoparticle Tracking Analysis (NTA) by NanoSight for the Measurement of Nanoparticles and Protein Aggregates. *Pharm. Res.* **2010**, *27*, 796−810.
(61) Wang, Q.; Zhao, H.; Qi, N.; Qin, Y.; Zhang, X.; Li, Y. Generation and stability of size-Adjustable Bulk Nanobubbles Based on periodic pressure Change. *Sci. Rep.* **2019**, *9*, 1118.
(62) Quach, N. V.-Y.; Li, A.; Earthman, J. C. Interaction of Calcium Carbonate with Nanobubbles Produced in an Alternating Magnetic Field. *ACS Appl. Mater. Interfaces* **2020**, *12*, 43714−43719.
(63) Fang, Z.; Wang, X.; Zhou, L.; Zhang, L.; Hu, J. Formation and Stability of Bulk Nanobubbles by Vibration. *Langmuir* **2020**, *36*, 2264−2270.
(64) Scott, T. A. Refractive index of ethanol-water mixtures and density and refractive index of ethanol-water-ethyl ether mixtures. *J. Phys. Chem.* **1946**, *50*, 406−412.
(65) Yusa, M.; Mathur, G. P.; Stager, R. A. Viscosity and compression of ethanol-water mixtures for pressures up to 40,000 psig. *J. Chem. Eng. Data* **1977**, *22*, 32−35.

https://dx.doi.org/10.1021/acsomega.0c05222
ACS Omega 2021, 6, 2873−2881